International Journal of Advanced Trends in Engineering and Management
(ISSN 2583-7052)

Vol. V, No. 06, pp. 18-25, June

Satellite Land-Use Scene Classification Using NGO-Optimized Densenet121 and Deep Belief Network Hybrid Model

Thomas Thangam[3]

[3]Assistant Professor, Department of Process Engineering, International Maritime College of Oman, National University of Science and Technology, Sohar, Sultanate of Oman,

Corresponding Author E-mail:

ABSTRACT: In recent days, remote sensing images (RSIs) are increasingly utilized for observing the changes in rural and urban areas and other wide range of applications such as disaster risk assessment, land use and environmental status. Since the resolution of RSIs is high with varying and wide data, clear illustration of RSIs is required. In geospatial analysis and remote sensing, Land use and Land-cover (LULC) classification based on deep learning (DL) has been emerged as effective approach that make use of Shapley additive explanations (SHAPs), which is a part of explainable artificial Intelligence (XAI). It aids in environmental monitoring, land management, mapping and land planning. Maintaining better accuracy in classification is necessary in various application domains. Hence in this work, a innovative structure that integrates Dense Net 121 and Deep Belief Network (DBN) model is employed to optimize parameters of Norther Goshawk Optimization (NGO) Algorithm, which aids in enhancing classification accuracy of classifier employed in this work. Effective feature extraction is performed using DenseNet121 through dense feature propagation, NGO optimize model parameters and improve quality of learned feature representation and DBN performs higher-level representations from extracted features. Outcomes achieved from simulation shows better results for NGO optimized DenseNet121 and DBN model than other conventional approaches.

Keywords: Land-use, Shapley additive explanation (SHAP), explainable AI (XAI), Northern Goshawk Optimization (NGO), DenseNet121 and Deep Belief Network.

1. Introduction

The technique of independently identifying remote sensing pictures into certain semantic labels based on environmental and geographic information contained in photos is known as remote sensing scene classification (RSSC). One of the important aspects of remote sensing picture interpretation is that each scene image is often linked to a single semantic term, such as building, forest, farming or road [1-3]. Land surveying often provides good results but it consumes more time and it is cost dependent. Hence, Earth observation (EO) data is performed to classify LULC [4,5] which is cost effective. In this work, DenseNet121 [6] is employed for classification of image which make the model more computationally effective, which aids the network to attain adaptive features and more durable. In [7], optimized and Explainable AI-based Framework for Land Use and Land cover Classification (OEF-LULC) is proposed for environmental and agricultural monitoring, but single dataset is used with 80/20 train-validation split. Hence in this work, NGO-optimized [8] using DenseNet121 and Deep Belief Network is proposed that classifies satellite scenes with better accuracy of classifier than other baseline approaches.

2. Recent Works

Meng Meng Li et al [2024] [8] has proposed a transformer need large scale training data, high complexity urban land use classification through scene wise unsupervised multisource domain adaptation with transformer in which the continuous use of source domain data is eliminated. Although it has high potential, high classification accuracy and strong stability, in computation and limited generalization to unseen region.

Yan-E-Hou et al [2023][9] have proposed end-to-end contextual spatial-channel attention network (CSCANet) to enhance performance in their classification and to study their hierarchical feature representations by integrating shallow object-level semantic information. Although accuracy is higher for classifying images, this model suffers from limited interpretability and large training data requirements.

Mohammed Aljebreen et al [2024][10] have proposed classification of Land use and Land cover using River Formation Dynamics Algorithm through deep learning in remote sensing images. The dense Efficient Net approach is employed for feature extraction. Although the simulation outcomes show higher accuracy than other approaches, it lacks convergence analysis, limited cross-dataset validation and high computational complexity.

Feng Xie et al [2025][11] have proposed scene-level detection model using Multiscale Feature Correlation Network for remote sensing images. Siamese-based multiscale feature corelation network (MSFCN) is employed for correlation extraction process. Although scene classification accuracy is higher, model suffers from sensitivity of images, limited generalization across datasets and high computational complexity.

Anastasios Temenos et al [2023][12] have proposed deep learning framework for Land use and land cover classification using Shapley additive explanation (SHAP). This model uses convolutional neural network (CNN) for satellite image classifications. Although prediction accuracy is higher, model suffers from correlations among image features, high computational and memory requirements and limited generability.

The contributions of the proposed work is given in the following;

- Integration of DenseNet121 for multi-layer spatial feature extraction with Deep belief Network (DBN) for land-use scene classification and high-level feature learning is developed.
- Optimizing the parameters of proposed deep-learning framework, NGO based algorithm is employed, which enhance classification performance.
- Higher accuracy is achieved using proposed framework than other conventional deep-learning framework.

The proposed work is explained in the following section.

3. Proposed Work Explanation

In the proposed methodology, image is fed as input to preprocessing unit which is performed using Gaussian filter that removes noise and blur from the input image given.

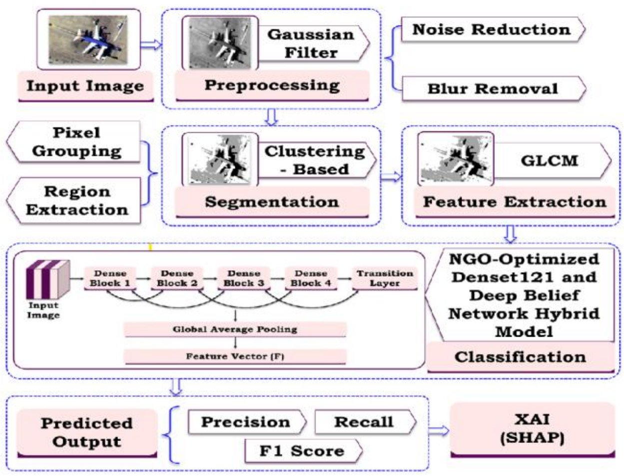

Figure 1: *Block diagram of proposed model*

After processing input image, noise-free image is subjected to clustering-based segmentation, in which pixel grouping and region extraction takes place. Feature extraction is performed to extract texture of image and feature representation which facilitates data classification. The selected features are subjected to classification performed using DBN classifier in which training of DBN classifier is performed using NGO optimized algorithm through DenseNet121 and predicted output is subjected to SHAP that improves interpretability of proposed model. The schematic diagram for proposed model is illustrated in Figure 1.

Gaussian Filter for preprocessing

In image processing, Gaussian filter is a critical tool that aids in noise reduction. Applying Gaussian kernel, filter provides central pixel that is more heavy than other regions, thereby reducing noise while preventing image structure. Filter scope and subsequent smoothing is controlled using Gaussian parameter. Using gaussian filter subtle noise pattern in image and blur iamages are removed thereby this filter is used in many image processing applications.

Clustering-Based Segmentation

Classification of different images requires different clustering approaches for processing images with better quality and reduced noise. Using cluster-based segmentation pixel grouping and region extraction is obtained. Clustering algorithm is used for minimizing sum of square in groups and it is stated as follows,

$$J(U,V,A) = \sum_{i=1}^{N} \sum_{j=1}^{C} (U_{ij})(D_{ij}) \qquad (1)$$

DenseNet121 architecture

From the conventional neural network, a predicted label is obtained which begins with capture of input image. Then image is subjected to network to provide expected label. Every subsequent convolutional layer produces a output feature except the first layer which receives input image. Since each layer is interconnected to each other in the network, it is collectively called as Densely Connected Convolutional Network.

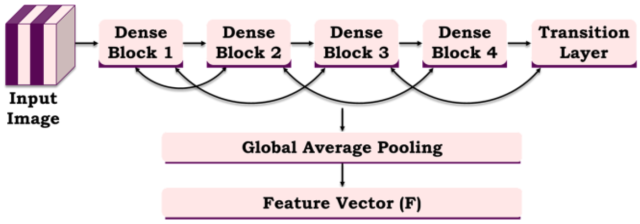

Figure 2: *Schematic diagram of Dense Net 121*

Deep Belief Network

DBN classifier performs classification of data using multiple layers of hidden units. The restricted Boltzmann layer undergoes unsupervised learning and supervised learning is performed using MLP layer. DBN architecture is shown in Figure 3.

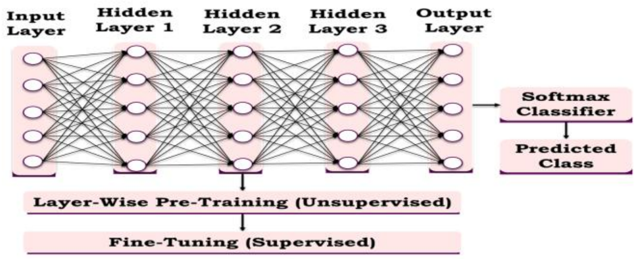

Figure 3: *Deep Belief Network architecture*

Northern Goshawk Optimization Algorithm

A medium-large hunter in family Accipitridae is named as norther goshawk, which hunts variety of prey such as mice, other birds prey, rabbits, squirrels, small and large birds, raccoons and even foxes. It follows two stages for hunting its prey namely, in the first stage it moves in high speed after identifying its prey and in its second stage, prey is hunted using short tail-chase process. In proposed algorithm, norther goshawk is the searcher members and each population member is indicated as solution for optimization problems that define specific value for decision variables. Each population is expressed as vector and these vectors form matrix. Initially population members are randomly selected in search space. Using equation (1) population matrix is initialized,

$$X = \begin{bmatrix} X_1 \\ \cdot \\ \cdot \\ X_i \\ \cdot \\ \cdot \\ X_N \end{bmatrix}_{N\times m} \quad (2)$$

Where X denotes northern goshawk population, N indicates population members numbers and X_i denotes ith proposed solution and number of problem variables is denotes as m. The flowchart for proposed NGO algorithm is represented in Figure 4

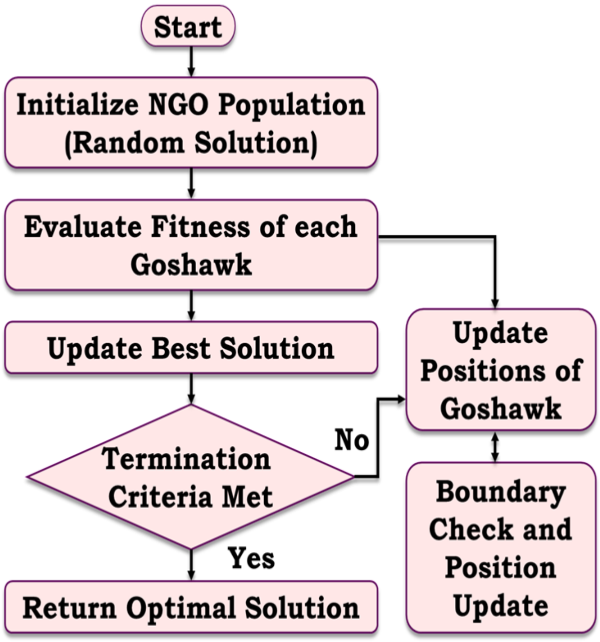

Figure 4: *Flowchart for NGO Algorithm*

The population members values attained using a vector function since each population member is defined as proposed solution to the problem and it is represented in equation (2),

$$F(X) = \begin{bmatrix} F_1 = F(X_1) \\ \cdot \\ \cdot \\ F_i = F(X_i) \\ \cdot \\ \cdot \\ F_N = F(X_N) \end{bmatrix}_{N\times 1} \quad (3)$$

Where F_i denotes objective function value attained for ith proposed solution and obtained objective function value vector is denoted as F. The best solution is decided using obtained objective function.

3.1 Mathematical Expressions and Symbols

The Mathematical expressions of proposed model are explained in the following. The proposed algorithms performance is evaluated using the metrics such as sensitivity, accuracy and specificity. Accuracy is stated as ratio of true measure to summation of observation given and it is indicated in equation (1) as,

$$D = \frac{I+J}{Total} \quad (4)$$

Where J indicates true negative, I indicate true positive and D indicates accuracy. The ratio of true positive rate to predicted observation rate, which is expressed in equation (2) as,

$$H = \frac{I}{I+V} \quad (5)$$

Where false negative is denoted as V and sensitivity is denoted as H. Ratio of true negative measure to unpredicted observations is termed as specificity and it is expressed in equation (3) as,

$$L = \frac{J}{J+U} \quad (6)$$

Where specificity is indicated as L and false positive rate is denoted as U.

4. Results and Discussion

This section provides details about outcomes of proposed model which is executed experimentally with given dataset. The dataset is accessed using the following link https://www.kaggle.com/datasets/apollo2506/landuse-_scene-classification and dataset name is given as satellite land dataset. Train image count is 8400 and test image count is 2100.

Train and test image per class is depicted in Figure 5(a), which is plotted between number of images vs class such as agriculture, beach, airplane, harbour, buildings, forest, river, runway, golf course, medium residential, storage tanks, tennis court and intersections. Train and test image split is depicted in Figure 5(b), which details that 20% of 2100 test image count and 80% of 8400 train image count is splitted.

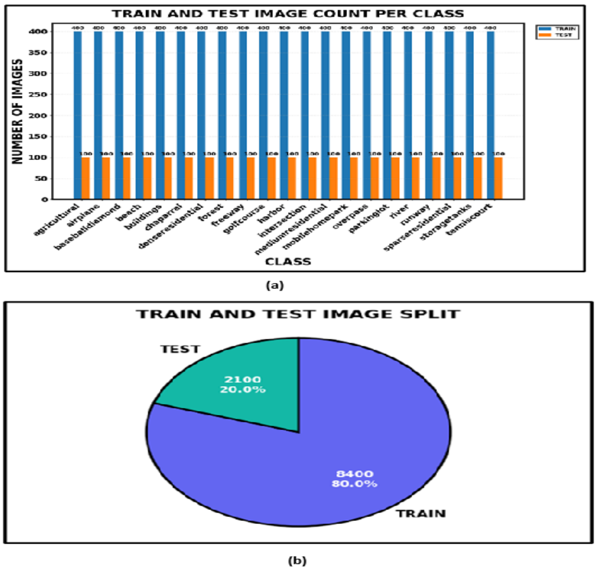

Figure 5: *Model Outcomes (a) Train and Test image per class (b) Tain and test image split*

Random train images from 8 classes such as intersection, mobilehomepark, parking lot, overpass, chaparral, forest, baseball diamond and medium residential is depicted in Figure 6(a). Random test images from 8 classes such as intersection, golfcource, sparse residential, runaway, buildings, river, forest and parking lot is depicted in Figure 6(b).

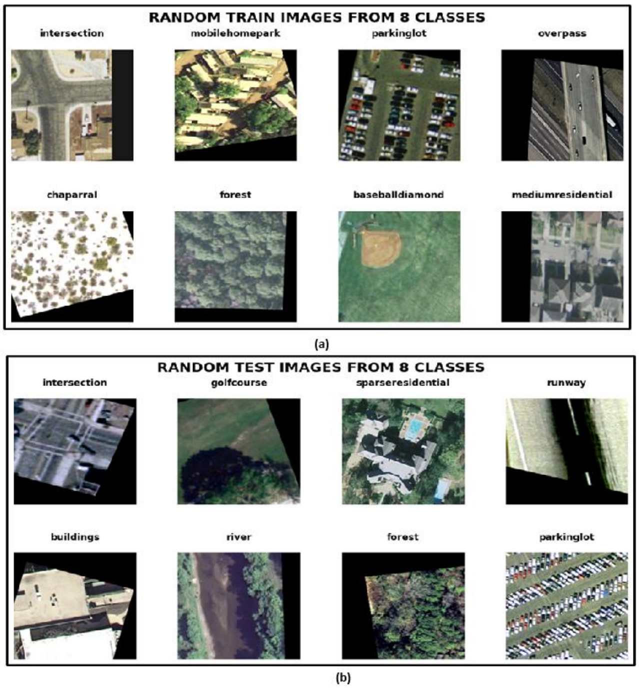

Figure 6: *(a) Random train images from 8 classes (b) Random test images from 8 classes*

In Figure 7, input image is depicted in Figure 7(a) which is image given as input to model. Resized image is shown in Figure 7(b), Grayscale image is shown in Figure7(c) and image which is filtered using Gaussian filter is shown in Figure 7(d).

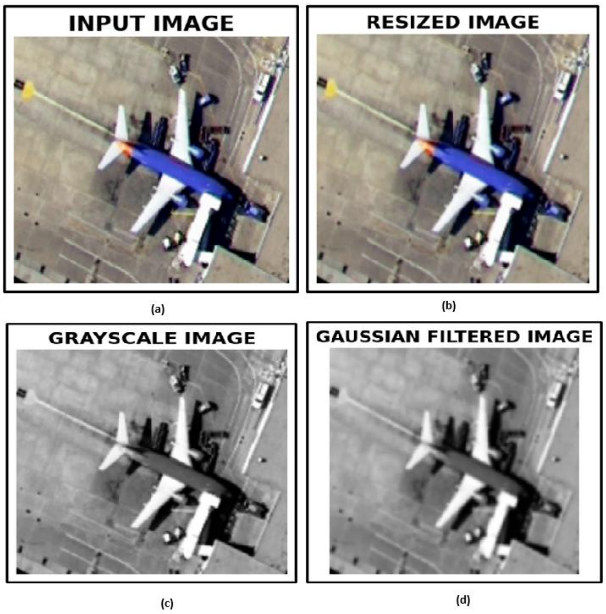

Figure 7: *(a) Input image (b) Resized image (c) Grayscale image (d) Gaussian Filtered Image*

Output image that is subjected to clustering-based segmentation is depicted in Figure 8(a) and GLCM feature image is depicted in Figure 8(b).

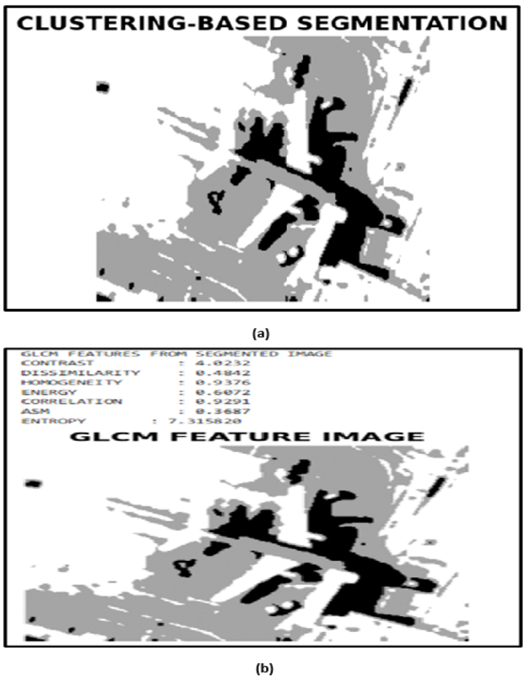

Figure 8: *Output image using (a) Clustering based segmentation (b) GLCM feature image*

The confusion matrix is depicted in Figure 9(a), which is plotted between actual class and predicted class. In Figure 9(b), ROC curve is plotted between true positive rate and false positive rate.

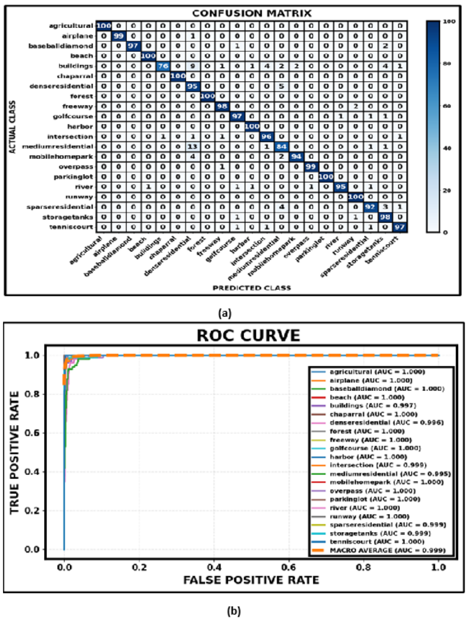

Figure 9: *Outputs (a) Confusion matrix (b) ROC curve*

The graph for training and testing accuracy is depicted in Figure 10(a), which is plotted between accuracy and epochs. Training and testing loss curve is depicted in Figure 10(b) which is plotted between loss and epoch values.

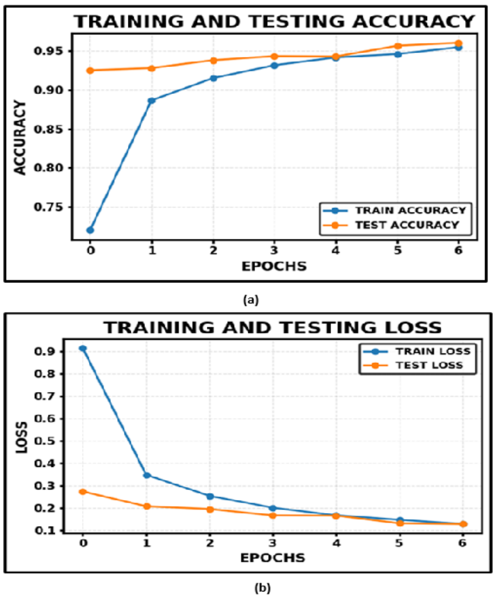

Figure 10: *Graph plotted for (a) Training and testing accuracy (b) Training and testing loss*

The performance metrics of proposed model is depicted in Figure 11, in which accuracy is 0.9605, precision of 0.9631, recall value of 0.9605, F1-score value of 0.9605, specificity of 0.9980, sensitivity of 0.9605, balanced accuracy of 0.9605, MCC value of 0.9585, Cohens Kappa value of 0.9585 and log loss of 0.1298.

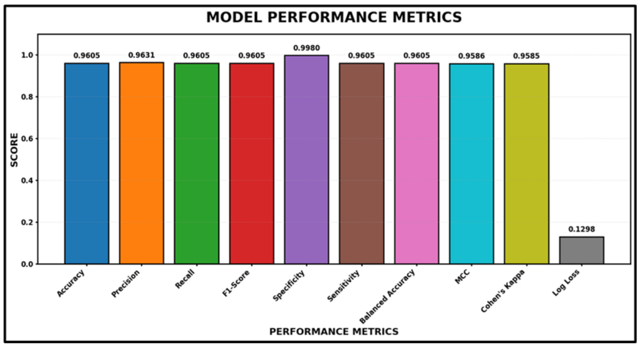

Figure 11: *Model performance Metrics*

In Figure 12(a), output predicted using dense Net 121 is shown, which gives details about class predicted and its confidence value. Forest class is predicted and its confidence value is 100%. Figure 12(b), gives details about output obtained using XAI-SHAP, in which forest class is subjected and its confidence value is 99.44%.

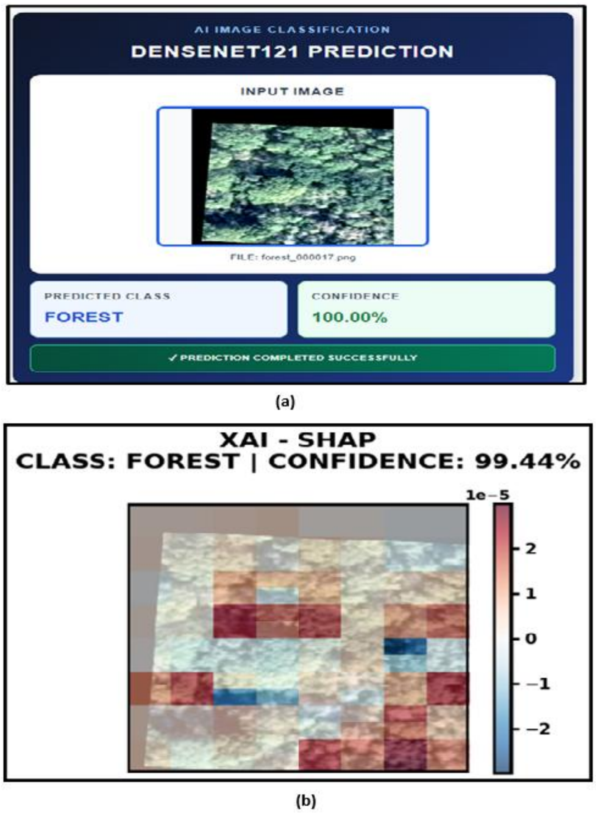

Figure 12: *Outputs using (a) Dense Net 121 (b) XAI-SHAP*

Comparison various classifiers such as Support Vector Machine (SVM), dense net 121 and proposed approach is shown in Figure 13. It details with 96% of accuracy, 96.3% precision, 96.05% recall value and 96.05% F1-measure.

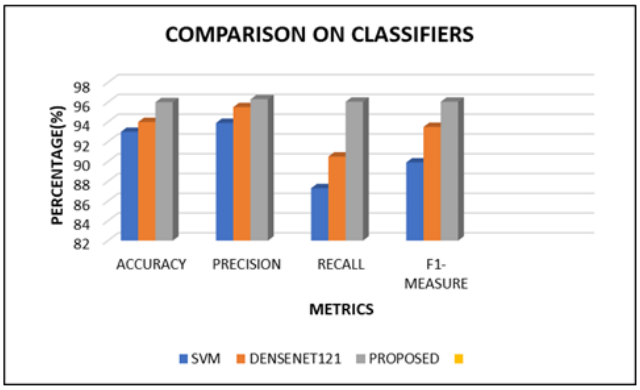

Figure 13: *Comparison graph on different classifiers*

5. Conclusion

In this proposed work, various stage of operations has been incorporated namely, denseNet121 for feature extraction, NGO-related parameter optimizer and DBN. The proposed approach combines DenseNet121 for hierarchical feature extraction with representation learning ability of DBN and selection and tuning of model parameters is performed using NGO optimization mechanism. This combination boosts classification efficacy across a variety of land-use categories by allowing model to incorporate both intricate patterns and differentiated geographic information identified in RSIs. This framework applies in agricultural monitoring, urban planning, environmental assessment, and large scale land-use mapping and resource management. However, proposed approach involves computational complexity, performance of the model is affected by dataset diversity, image resolution and spatial conditions. Future research direction is focused on evaluating this model with larger dataset incorporating high spectral information and improving interpretability of classification decision by investigating XAI.

References

1. Ziwe Li; Weiming Xu; Shiyu Yang; Juan Wang; Hua Su; Zhanchao Huang; Sheng Wu, Year: 2024, “A Hierarchical Graph-Enhanced Transformer Network for Remote Sensing Scene Classification”, In IEEE Journal of Selected Topics in Applied Earth Observations and Remote Sensing, Vol: 17, pp. 20315-20330.
2. Andres J Sanchez-Fernandez; Sergio Moreno-Álvarez; Juan Antonio Rico-Gallego; Siham Tabik, Year: 2024, “Self-Supervised Learning on Small In-Domain Datasets Can Overcome Supervised Learning in Remote Sensing”, In IEEE Journal of Selected Topics in Applied Earth Observations and Remote Sensing, Vol: 17, pp. 12797-12810.
3. Chao Tao; Ji Qi; Mingning Guo; Qing Zhu; Haifeng Li, Year: 2023, “Self-Supervised Remote Sensing Feature Learning: Learning Paradigms, Challenges, and Future Works”, In IEEE Transactions on Geoscience and Remote Sensing, Vol: 61, pp. 1-26.
4. Kangkai Lou; Mengmeng Li; Fashuai Li; Xiangtao Zheng, Year: 2024, “Integrating Local-Global Structural Interaction Using Siamese Graph Neural Network for Urban Land Use Change Detection from VHR Satellite Images”, In IEEE Transactions on Geoscience and Remote Sensing, Vol: 62, pp. 1-17.
5. Yi Wang; Nassim Ait Ali Braham; Zhitong Xiong; Chenying Liu; Conrad M. Albrecht; Xiao Xiang Zhu, Year: 2023, “SSL4EO-S12: A large-scale multimodal, multitemporal dataset for self-supervised learning in Earth observation [Software and Data Sets]”, IEEE Geosci. Remote Sens. Mag, Vol: 11, No: 3, pp. 98–106.

6. T. S. Arulananth; S. Wilson Prakash; Ramesh Kumar Ayyasamy; V. P. Kavitha; P. G. Kuppusamy; P. Chinnasamy, Year: 2024, “Classification of Paediatric Pneumonia Using Modified DenseNet-121 Deep-Learning Model”, In IEEE Access, Vol: 12, pp. 35716-35727.
7. Ruaa A. Al-Falluji; Marwan Ali Albahar, Year: 2026, “OEF-LULC: An Optimized and Explainable AI-Based Framework for Land Use Land Cover Classification”, In IEEE Access, Vol: 14, pp. 38745-38757.
8. Brenton A. Wilder; Christine M. Lee; Adam Chlus; Hans-Peter Marshall; Jodi Brandt; Alicia M. Kinoshita; Josh Enterkine; Thomas Van Der Weide; Nancy F. Glenn, Year: 2024, “Computationally Efficient Retrieval of Snow Surface Properties From Space borne Imaging Spectroscopy Measurements Through Dimensionality Reduction Using K-Means Clustering”, In IEEE Journal of Selected Topics in Applied Earth Observations and Remote Sensing, Vol: 17, pp. 8594-8605.
9. Mengmeng Li; Congcong Zhang; Wufan Zhao; Wen Zhou, Year: 2024, “Cross-Domain Urban Land Use Classification via Scene wise Unsupervised Multisource Domain Adaptation With Transformer”, In IEEE Journal of Selected Topics in Applied Earth Observations and Remote Sensing, Vol: 17, pp. 10051-10066.
10. Yan-E. Hou; Kang Yang; Lanxue Dang; Yang Liu, Year: 2023, “Contextual Spatial-Channel Attention Network for Remote Sensing Scene Classification”, In IEEE Geoscience and Remote Sensing Letters, Vol: 20, pp. 1-5.
11. Mohammed Aljebreen; Hanan Abdullah Mengash; Mohammad Alamgeer; Saud S. Alotaibi; Ahmed S. Salama; Manar Ahmed Hamza, Year: 2024, “Land Use and Land Cover Classification Using River Formation Dynamics Algorithm With Deep Learning on Remote Sensing Images”, In IEEE Access, Vol: 12, pp. 11147-11156.
12. Feng Xie; Zhongping Liao; Jianbo Tan; Zhiguo Hao; Shining Lv; Zegang Lu; Yunfei Zhang, Year: 2025, “MSFCN: A Multiscale Feature Correlation Network for Remote Sensing Image Scene Change Detection”, In IEEE Journal of Selected Topics in Applied Earth Observations and Remote Sensing, Vol: 18, pp. 8275-8299.
13. Anastasios Temenos; Nikos Temenos; Maria Kaselimi; Anastasios Doulamis; Nikolaos Doulamis, Year: 2023, “Interpretable Deep Learning Framework for Land Use and Land Cover Classification in Remote Sensing Using SHAP”, In IEEE Geoscience and Remote Sensing Letters, Vol: 20, pp. 1-5.